Journal of Photochemistry & Photobiology A: Chemistry 375 (2019) 48–53

Contents lists available at ScienceDirect

Journal of Photochemistry & Photobiology A: Chemistry

journal homepage: www.elsevier.com/locate/jphotochem

Full Length Article

Photoresponsive azobenzene ligand as an efficient electron acceptor for luminous CdTe quantum dots

Shomaila Saeed[a], Jun Yin[c], Muhammad Adnan Khalid[a], Pervaiz Ali Channar[a], Ghulam Shabir[a], Aamer Saeed[a], Muhammad Arif Nadeem[a], Cesare Soci[b], Azhar Iqbal[a,b,*]

[a] Department of chemistry, Quaid-I-Azam University Islamabad, 45320, Pakistan
[b] Division of Physics and Applied Physics, School of Physical and Mathematical Sciences, Nanyang Technological University, 21 Nanyang Link, 637371, Singapore
[c] Division of Physical Sciences and Engineering, King Abdullah University of Science and Technology, Thuwal, 23955-6900, Saudi Arabia

ARTICLE INFO

Keywords:
CdTe quantum dots
Photochrome
Fluorophore
Electron transfer
FRET
Luminescent probe

ABSTRACT

Surface modified semiconductor quantum dots (QDs) with a tunable photoluminescence (PL) are particularly desirable for many photo-responsive devices. In a step forward towards this goal using 3-mercaptopropionic acid (MPA) the CdTe QDs of different sizes are synthesized. The MPA not only controls the size of the QDs but its dense shell around the surface also passivates the surface traps. Consequently, the CdTe QDs exhibit narrow emission with full-width at half-maximum (FWHM) of ~0.3 eV. These QDs are attached to (E)-4-((3-formyl-4-hydroxyphenyl) diazenyl) benzoic acid (FHDBA) to fabricate a photochrome-fluorophore assembly. Ultraviolet (UV) irradiation induces trans-cis isomerization in FHDBA. Upon storing FHDBA in dark for ~30 min, it completely reverts to trans-isomer. After photoisomerization the absorption band (n – π* transition) of cis-isomer of FHDBA overlaps with the emission band of CdTe QDs. Following UV excitation photoinduced electron transfer (ET) from conduction band (CB) of CdTe QDs to the LUMO of the cis-isomer of FHDBA quench the fluorescence of QDs by ~16 times. Förster resonance energy transfer (FRET) may also quench the fluorescence but its contribution is minor. The photoinduced reversible trans-cis interconversion of FHDBA followed by ET in QDs-FHDBA assembly and the dual function of MPA as coupling strategy may open the avenues to design QDs luminescent photoswitchable probes for biomedical and energy storage applications.

1. Introduction

Semiconductor QDs have fueled a great deal of interest for their applications in photovoltaics [1], biomedical imaging [2–5] and information processing [6,7]. The QDs display narrow emission bands located near IR and visible region of the solar spectrum [8]. They exhibit long photoluminescence (PL) lifetimes and photo-bleaching resistance [9]. This property makes them a suitable candidate to be used as an alternative to organic dyes [10]. Band gap tuning ability of II—VI semiconductor QDs over a wide energy range may offer many advantages over the silicon [11]. Bulk CdTe has band gap of 1.5 eV [12]. The emission band of CdTe nanocrystals is narrow and symmetric and can be adjusted precisely across the visible and near IR region by controlling the size and the composition of the elemental constituents. The CdTe nanostructures have revealed their applications in the field of sensing [13], optoelectronics [14], catalysis [15], electrode materials for lithium ion battery [16], field emission emitter [17] and as luminescent probes [18].

The photochromic molecules have the ability to transform between two reversible isomers upon absorption of a photon of electromagnetic radiation. Common reversible processes of transformation involve the trans – cis isomerization, ring opening-closing mechanism, proton transfer and electron transfer [19]. Aforementioned processes alter the electronic structure and change the geometry, dipole moment and absorption coefficient of the photochromic molecules [19]. Optical control of isomerization of azobenzene compounds has been utilized in diverse applications [20–24]. The ability of photoisomerization of some other relevant photochromic molecules have also been utilized as photoswitches to modulate the fluorescence of the fluorophores [19,25–27].

This report describes the fabrication of a photochrome-fluorophore assembly that consists of a new type of photoresponsive azobenzene derivative FHDBA. It works as a photo-switch due to reversible trans-cis isomerization. The QDs are attached to FHDBA by 3-mercaptopropionic acid (MPA). The MPA has a dual function i.e., it stabilizes and controls the size of the QDs and as well as it works as anchoring group for

* Corresponding author.
E-mail address: aiqbal@qau.edu.pk (A. Iqbal).

https://doi.org/10.1016/j.jphotochem.2019.02.007
Received 10 November 2018; Received in revised form 20 December 2018; Accepted 5 February 2019
Available online 12 February 2019
1010-6030/

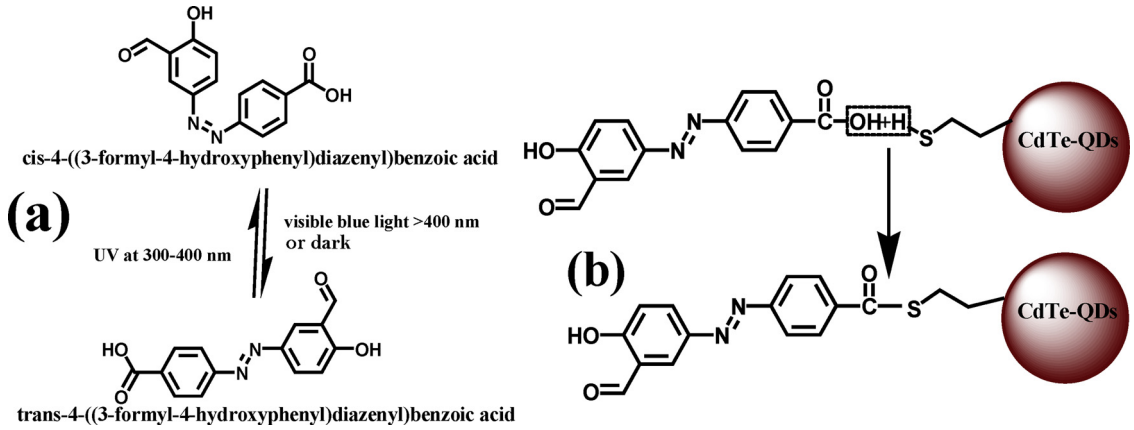

Scheme 1. (a) Trans-cis interconversion of FHDBA, (b) mechanism of attachment of CdTe QDs to FHDBA.

attachment to FHDBA. Photo-induced trans-cis interconversion of FHDBA (Scheme 1a) quench the emission of CdTe QDs by electron transfer (ET) from the CB of CdTe QDs to the lowest unoccupied molecular orbital (LUMO) of the cis isomer of FHDBA. The CdTe QDs are attached to FHDBA by following the procedure given in our previous publication [28] and is displayed by Scheme 1. The attachment of CdTe QDs with FHDBA occurs through carboxylate chelating bidentate interactions [29,30].

2. Experimental

2.1. Materials

All chemicals used were as purchased without further purification. The $CdCl_2{\cdot}2.5H_2O$ (99%) was purchased from Sigma Aldrich; tellurium powder (99.9%) was purchased from Alfa Aesar and hydrazinium hydroxide (99.5%) was purchased from Riedel de Haen. Salicylaldehyde (99.8%), aniline (99.5%), 3-mercaptopropionic acid (99.5%), methanol (99.9%), ethanol (99.9%), acetone (99.5%), n-hexane (99.5%) were purchased from Merck. Dual deionized water was employed as a solvent during the synthesis process.

2.2. Preparation of CdTe QDs

Synthesis of CdTe is problematic as compared to other II – VI metal chalcogenides because it needs to be pretreated to prepare unstable tellurium precursor (NaHTe or H_2Te), which is susceptible to oxidation and to avoid oxidation, we perform the experiment under nitrogen atmosphere. Briefly, $NaBH_4$ (0.1284 g), deionized water (10 mL), tellurium powder (0.076 g) and hydrazinium hydroxide (2 mL) were taken in three necked round bottom flask and the precursors were mixed by gentle stirring at room temperature. Throughout the reaction, high purity nitrogen was injected into the flask to remove the oxygen and shield the fresh NaHTe against oxidation. Approximately 4 h later, the black Te precursor was used up and the subsequent NaHTe in translucent purple supernatant liquid was produced that was utilized for the synthesis of CdTe QDs.

The synthesis of CdTe QDs was performed in inert conditions i.e. in nitrogen environment. **$CdCl_2{\cdot}2.5H_2O$** is used as Cd^{+2} precursor and 3-mercaptopropionic acid (MPA) was used as a capping/stabilizing agent for CdTe QDs. The molar ratio of Cd^{2+}, Te^{2-}, and MPA was taken 1:2:1, 2, 3, 4, 5, respectively. Te^{2-} ion precursor (freshly synthesized) amount was taken double than Cd^{+2} ion precursor, because **severe conditions were required for its reduction**. Cd^{+2} ion precursor solution was made by stirring **$CdCl_2{\cdot}2.5H_2O$** and MPA solution together, this made the solution turbid indicating the formation of Cd (II)–MPA complex that fades out by adding ammonia solution to establish pH = 11. Three-necked flask was used for synthesis process with close-fitting and deaerated with N_2 aeration for 30 min. During mixing, NaHTe solution was added gradually. The mixture was heated at 130 °C and refluxed for 18 h. The size of the QDs was controlled by changing the concentration of MPA. The variation of colour in the colloidal mixture of the CdTe QDs was evidently seen by naked eye, which changes from pale yellow to bright red solution. After synthesis, the CdTe QDs were cooled down to room temperature, centrifuged, washed with distilled water, methanol, ethanol, n-hexane and acetone and desiccated at room temperature. The QDs were evenly dispersed in polar solvents but aggregated in non-polar solvents. The MPA under basic conditions (pH = 11) is used to regulate the size of CdTe QDs and it acts as a stabilizer as well.

2.3. Preparation of 4-((3-formyl-4-hydroxyphenyl) diazenyl) benzoic acid (FHDBA)

The FHDBA has been synthesized by following the method given in Shabir. G. et al. [31], which involves a reaction between aniline and salicylaldehyde using diazo solution at 0–5 °C for coupling reaction. The chemical structure of FHDBA and the reaction mechanism of synthesis is given in reaction Scheme 2.

2.4. Preparation of QDs-FHDBA assembly

For the fabrication of QDs-FHDBA assembly the MPA capped CdTe QDs has been attached to FHDBA. The MPA controls the size and works as surface modifier for CdTe QDs. The attachment of FHDBA with MPA capped CdTe QDs is achieved by thiol linkage through a condensation reaction [28], Scheme 1b. For this purpose, **1 mL of MPA (5 M)** capped CdTe QDs solution in ethanol (10 mL), and a 1μM solution of FHDBA in ethanol (10 mL) were prepared. Both these solutions were mixed, stirred and heated at 80 °C for 48–72 h, thereafter a dark red solution

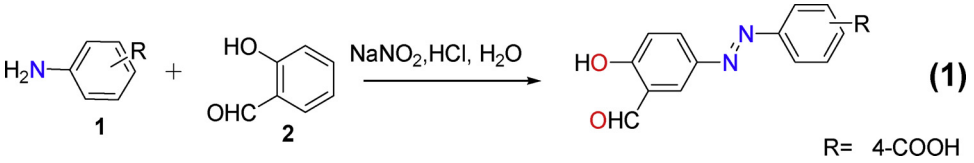

Scheme 2. Reaction mechanism for the synthesis of FHDBA.

was produced.

2.5. Methods

The morphological investigation of CdTe QDs has been conducted by using JEOL, JEM-2010 high-resolution transmission electron microscope (HRTEM). The information regarding the crystal structure of CdTe QDs is obtained by powder X-rays diffraction (XRD) analysis. The XRD analysis of CdTe QDs were performed by using the 3040/60, X'Pert Pro equipped with copper K_α radiation source having nickel metal foil filters in the 2θ range of 10–70°. Shimadzu UV-1601 spectrophotometer was used to conduct UV–vis absorption measurements at room temperature. All the samples were analyzed using the quartz cuvettes. Steady-state photoluminescence (PL) and time-resolved PL measurements were conducted by Pico Quant Fluo Time-300 spectrophotometer. The PL was measured following pulsed LED laser (PLS-300) excitation. The excitation pulse is centered at 306 nm with a pulse duration of ˜416 ps and the pulse energy is ~0.077 pJ. The CdT samples were dispersed in absolute ethanol for PL measurements were conducted at room temperature. Density functional theory (DFT) calculations were performed using Vienna ab initio simulation package (VASP), for further details please see section 3, supporting information.

3. Results and discussion

Transmission electron microscope (TEM) images of CdTe QDs capped with 5 M MPA (Fig. S1 (a) and (b), SI) suggest that QDs average (Fig. 1 (b)) diameter is ~1–3 nm. The QDs size revealed by HRTEM images is in agreement with the size predicted by XRD (Fig. S2, eq. 1, SI) and UV/Vis absorption measurements (eq. (2), SI). The large-area and HRTEM images (Fig. S1 (a) and S1 (b)) suggest the QDs are mainly monodisperse with minimal aggregation. Fig. 1 displays HRTEM image with fast Fourier transform (FFT) pattern in the inset. The FFT pattern demonstrates that the QDs exists in cubic phase with inter-planar distance of about 3.38 Å between (111) planes, thus consistent with the reference card, JCPDS No. 65-1046 [32], which predicted inter-planar distance of 3.43 Å and is in good agreement with the XRD measurements. The little variation in the diffraction patterns of XRD (Fig. S2, SI) is because of distortions in the crystal-lattice due the very finite size of the QDs. The peaks at 2θ values of 24.7°, 40.6° and 49.6° correspond to crystallographic planes of (1 1 1), (2 2 0) and (3 1 1) suggesting that CdTe QDs exist in cubic phase. Further, it reveals that as the concentration of MPA is increased the peaks broaden, indicating that the size of the QDs decreases.

The decrease in the size of CdTe QDs by increasing the concentration of MPA is also demonstrated in UV–vis absorption measurements, where a blue shift in the excitonic peak of CdTe QDs has been observed.

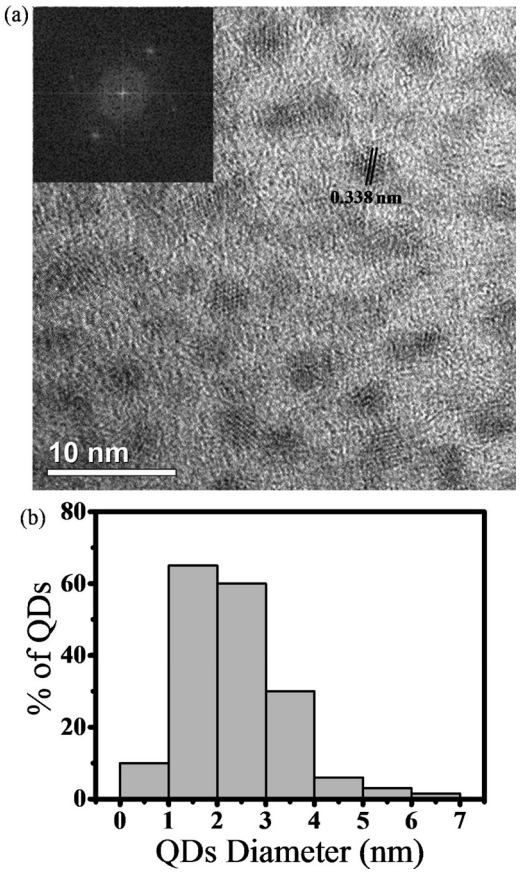

Fig. 1. (a) HRTEM image of CdTe QDs capped with 5 M MPA, inset displays the FFT pattern and (b) estimated size distribution of QDs capped with 5 M MPA by HRTEM.

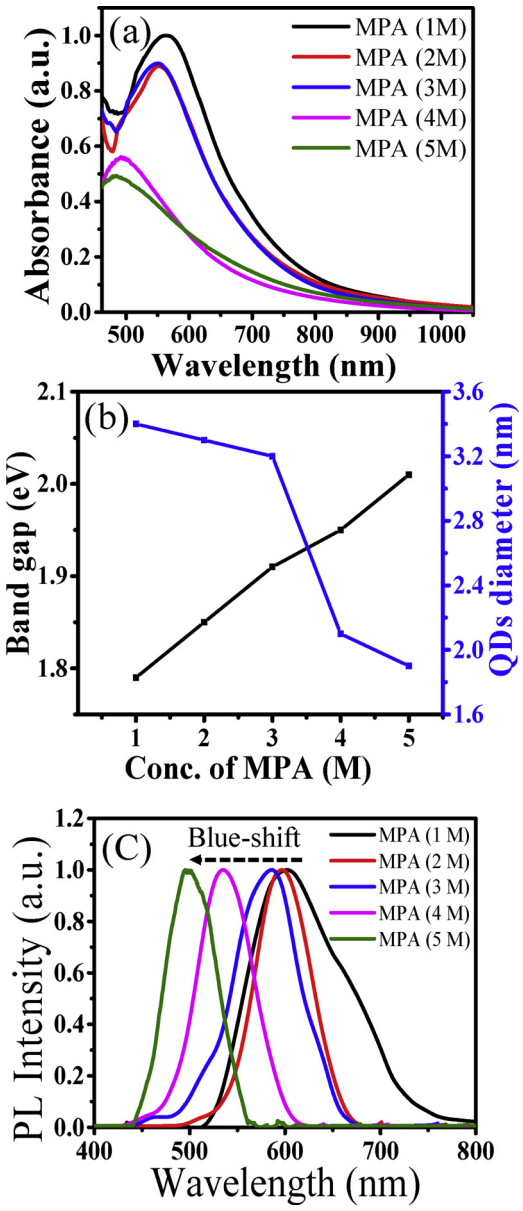

Fig. 2. (a) UV–vis absorption spectra of MPA capped CdTe QDs, (b) relationship between band gap and the size of CdTe QDs with varying concentration of MPA, (c) steady-state PL spectra of CdTe QDs containing various amonts of MPA, after excitation at 306 nm.

The peaks maxima of CdTe QDs (Fig. 2a) are significantly blue shifted as compared to the bulk [12] CdTe. The size of the QDs is estimated from absorption spectra by using Yu et al. model [33], presented in eq 1.

$$D = (9.8127 \times 10^{-7})\lambda^3 - (1.7147 \times 10^3)\lambda^2 + (1.0064)\lambda - 194.84 \quad (1)$$

where D is the size of the QDs and λ is the wavelength of the first excitonic peak. The calculated sizes range from 1.9 to 3.4 nm, thus in strong agreement with the sizes measured by HRTEM. The band gap of CdTe QDs is estimated by Tauc method [34] (Fig. S3 (a) & (b), eq. (2), SI). The diameter of QDs decreases and the band gap increases linearly by increasing the concentration of MPA (Fig. 2b). Following pulsed LED laser excitation at 306 nm, the Stokes shifted PL exhibits an incredible blue shift ~0.45 eV (Fig. 2c) as the concentration of MPA increases from 1 to 5 M. It further reveals that for higher concentration of MPA, the PL spectra of QDs is much narrower. **This can be attributed to the improvement of crystallization and the QDs population with the homogeneous size**. The CdTe QDs containing 5 M capping agent are attached to FHDBA and the effect of FHDBA on the PL is discussed in the forthcoming paragraphs.

The chemical structure of the synthesized FHDBA was confirmed by ^{1}H NMR, ^{13}C NMR (Figs. S4 (a) & 4 (b), SI). The MPA capped CdTe QDs attach to FHDBA by condensation reaction through the thiol linkage. The confirmation about the mode of attachment of QDs with FHDBA and fabrication of QDs-FHDBA assembly is done by FTIR spectra Fig. S4, SI. The spectra (Figs. 5 (a), 5 (b) & 5 (c), SI) confirm that QDs attach to FHDBA by developing thiol linkage through condensation reaction.

Fig S5 (a), SI shows FTIR spectrum of FHDBA describing strong absorption features at about 3392 cm^{-1} due to stretching vibrations of hydroxyl group and at 3015 cm^{-1} for sp^2 C–H of aromatic rings. The presence of sharp and strong absorptions feature at 1740-1622 cm^{-1}, indicates the presence of carbonyl groups in the molecule. Fig S5 (b) shows FTIR spectrum of CdTe QDs with a clear 2552 cm^{-1} absorption feature showing the presence of S–H **link and the absence of absorption feature of OH at 3390 cm^{-1} is an indication of MPA capping through COO – link. FTIR spectrum (Figure S5(c), S1) shows that MPA capped CdTe QDs were attached to FHDBA by -CS- bond through a condensation reaction as described in** Scheme 1**. Absence of** S–H **peak at 2552 cm^{-1} after attachment in Fig S5 (c) was an evidence in this regard that FHDBA-CdTe QDs attachment was done through thiol linkage.**

The UV–vis absorption spectrum of FHDBA (Fig. 3a (i)) in ethanol exhibits two strong features at 341 nm and 531 nm. The absorption feature at 341 nm can be attributed to π – π* transition, while peak at 531 nm is due to n – π* transition in the trans-isomer of FHDBA. The UV irradiation with UV lamp at 300 nm (half an hour) encouraged the trans → cis isomerization of FHDBA, as a result a strong decrease in the absorption intensity of π – π* transition at 341 nm has been observed with a concomitant increase in the absorption intensity of n – π* transition at 531 nm (Fig.3a (ii)). The peak at 531 nm of cis-isomer is slightly blue shifted. This is due to the attachment of electron-withdrawing group −COOH to the para position of one benzene ring of the azo moiety. The presence of electron donating groups at the ortho and para positions cause a red shift in n – π* transition in cis-isomer but increase the cis – trans transformation rate [35]. The slight blue shift in this case is advantageous because it increases the lifetime of cis-isomer and can make it more efficient switch. The lifetime of cis-isomer of FHDBA is ~30 min. The lifetime is estimated by photoconverting the FHDBA from trans - cis at 300 nm A reversible cis – trans transformation of FHDBA is monitored upon storing it in the dark. A complete recovery of trans-isomer is obtained in half an hour, as demonstrated by Fig. 3b, which displays the change in absorbance at 531 nm as a function of time. The long lifetime of cis-isomer of FHDBA has demonstrated itself by quenching the PL of CdTe QDs by ~16 times. Details of these findings will be discussed in forthcoming paragraphs.

In order to engineer QDs-FHDBA assembly the CdTe QDs capped with 5 M MPA are attached to FHDBA. **After attachment a slight red shift of π – π* transition at 341 nm (Fig. 3a (iii)) can be associated with deprotonation of hydroxyl group** [36]. In addition, a small feature in the absorption spectrum of QDs-FHDBA appears at 475 nm indicating an ET from QDs to FHDBA. To engineer QDs-FHDBA assembly, the selection of CdTe QDs containing 5 M MPA is made because its PL spectrum exactly overlaps with the absorption band of the cis-isomer of FHDBA, green trace Fig. 3a (iv).

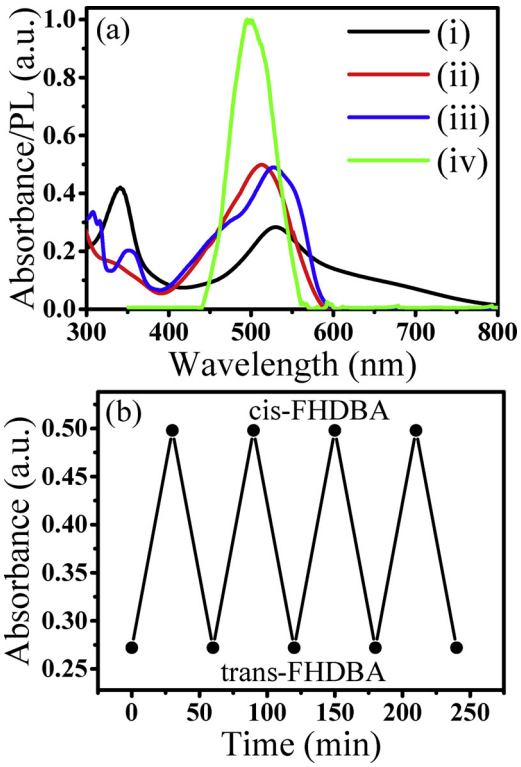

Fig. 3. (a): (i) UV–vis absorption spectrum of FHDBA, (ii) UV–vis absorption spectrum of FHDBA after UV irradiation at 300 nm (half an hour), (iii) UV–vis absorption spectrum of QDs attached FHDBA, (iv) PL spectrum of CdTe QDs capped with 5 M MPA; (b) change in absorbance at 531 nm (n – π* transition) after UV (300 nm) irradiation and at 531 nm and upon storing in dark as a function of time.

Following excitation at 306 nm, the PL spectrum of CdTe QDs (Fig. 4a, black trace) peaks at 500 nm with a very narrow emission band (FWHM ~0.3 eV). The red trace in Fig. 4a corresponds to the QDs-FHDBA assembly i.e. CdTe QDs capped with 5 M MPA attached to FHDBA. As it is clear that PL of the QDs is strongly quenched and the PL peak intensity has been decreased by ~16 times. The reason of fluorescence quenching can be attributed to the trans – cis interconversion of FHDBA followed by ET from CdTe QDs to FHDBA. The absorption band of the cis-isomer of FHDBA (n – π* transition) overlaps with the CB of the CdTe QDs. Due this overlap, ET from the CB of the QDs to the LUMO of FHDBA occurs and it causes a huge decrease in the PL intensity of the QDs. The fluorescence quenching, following ET from fluorophore to photochrome has also been observed in other relevant photo-responsive systems [27,28,37,38]. It is important to mention here that the steady-state PL of FHDBA in ethanol has also been conducted after excitation at 306 nm (Fig. S6 (a), SI). The marked differences of the PL spectrum of FHDBA as compared to QDs-FHDBA strongly suggest that PL of QDs have been quenched by following ET from QDs to FHDBA.

The PL decay kinetics is displayed in Fig. 4b. Shortening in PL lifetime of QDs attached to FHDBA is observed. Both the CdTe QDs and QDs-FHDBA samples exhibit a non-exponential behavior of PL decay. Bi-exponential decay function best fits the PL kinetics of CdTe QDs, while tri-exponential decay function gives a best fit for PL decay

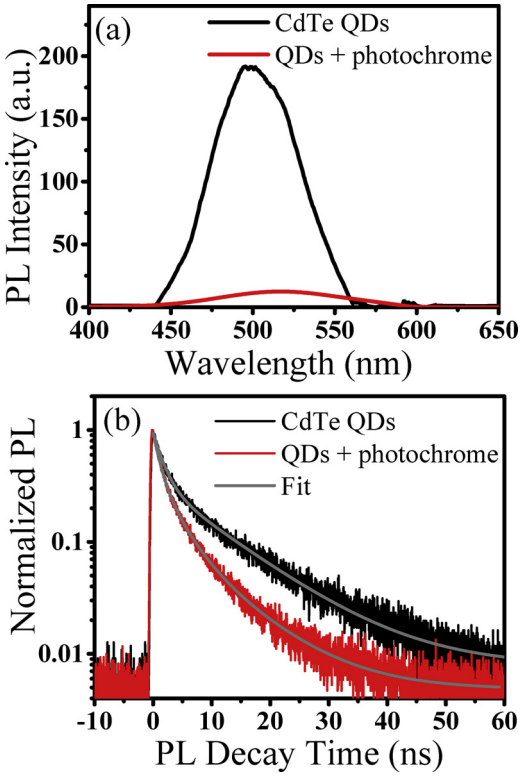

Fig. 4. (a) Room temperature steady-state PL spectra of bare and FHDBA attached CdTe QDs, (b) time-resolved PL kinetics at 500 nm of bare CdTe QDs and FHDBA attached QDs.

kinetics of the QDs-FHDBA assembly. The time constants extracted from the best fits for the PL decay kinetics of QDs are 1.72 ns and 11.17 ns, and 1.05 ns, 3.19 ns and 9.3 ns for QDs-FHDBA (table 1, SI). The PL of QDs-FHDBA system decays much faster at early timescales than the PL of QDs only, confirming the ET from the QDs to the FHDBA. These finding are in consistent with the strong PL quenching in QDs-FHDBA system. The PL lifetime of MPA capped CdTe QDs is slightly shorter as compared to the CdTe QDs prepared by other stabilizing/capping agents [39,40]. This suggests that the photophysical properties of CdTe QDs are greatly influenced by the capping ligands. It is important to highlight here that fluorescence can be quenched both by energy and charge transfer processes. The occurrence of Dexter type energy transfer is highly unlikely to be operative here because the capping agent MPA could offer a significant hindrance for the overlap of donor and acceptor wave functions. However, Förster resonance energy transfer (FRET) [41,42] can equally be operative in our QDs-FHDBA system due the overlap of the absorption band of the acceptor and the emission band of the donor. The efficiency (E) of FRET is estimated by eq. (2),

$$E = 1 - \frac{\tau_{DA}}{\tau_D} \quad (2)$$

where, τ_{DA} and τ_D are the average fluorescence lifetimes (1/e) of the donor in presence (1.90 ns) and in the absence (3.2 ns) of the acceptor, respectively. The estimated FRET efficiency is ~40% suggesting that both ET (~60%) and FRET are possible but FRET contribution is minor.

To further understand the possible electron injection from CdTe QDs into cis-FHDBA, we performed density functional theory (DFT) calculations on the $Cd_{43}Te_{43}$ clusters with both MPA-bidentate chelating and MPA-bidentate bridging carboxyl groups to micmic experimental 5 M capped MPA CdTe QDs system (see the details in *Computational Methods* section 3, SI). The calculated projected density of states (PDOS) is shown in Fig. 5. Our proposed cis-FHDBA/MPA linked $Cd_{43}Te_{43}$ cluster can achieve an efficient ET due to strong electronic couplings between LUMO level of cis-FHDBA and $1s_{electron}$ state of $Cd_{43}Te_{43}$ cluster, especially in the MPA-bidentate chelating case due to the formation of hybrid state. Note that we can exclude the cis-FHDBA directly linked $Cd_{43}Te_{43}$ clusters, since the opposite ET occurs from cis- FHDBA to CdTe QDs, because of LUMO level of cis- FHDBA is above $1s_{electron}$ state of $Cd_{43}Te_{43}$ cluster (see PDOS in Fig. S7, SI).

4. Conclusions

Our measurements demonstrated that FHDBA was an excellent photoresponsive molecule, the UV exposure at 300 nm caused trans-cis isomerization and upon storing in the dark, it was completely reversed to trans-isomer. The fluorescence quenching of CdTe QDs in QDs-FHDBA assembly following UV excitation demonstrated that FHDBA was an excellent electron acceptor in cis-form. ET from CB of the QDs to the LUMO of the cis-isomer of FHDBA mainly caused the fluorescence quenching. The signature of fluorescence quenching by FRET was also observed but its contribution was minor. The CdTe QDs coupled photoresponsive FHDBA by MPA demonstrated efficient electron/energy transfer following UV excitation. The coupling strategy and photoresponsive behavior of CdTe QDs-FHDBA assembly may lead to design

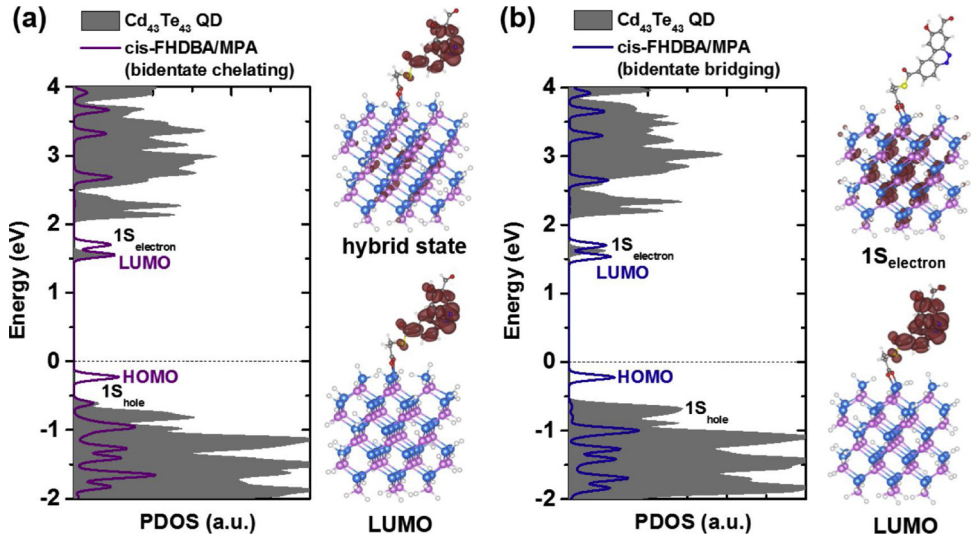

Fig. 5. PDOS and electronic charge density distributions for frontier orbitals of MPA/cis-FHDBA linked $Cd_{43}Te_{43}$ QD with a (a) bidentate chelating and (b) bidentate bridging carboxyl group.

luminescent probes for photoactivatable devices.

Acknowledgements

We highly acknowledge the financial support of Higher Education Commission (HEC) of Pakistan for the equipment/research grant (20-3071/NRPU/R&D/HEC/13). The authors are highly thankful to Dr. Zhang Zhicheng and Dr. Faisal Saleem, School of Materials Science and Engineering, Nanyang Technological University of Singapore for their help with HRTEM analysis.

Appendix A. Supplementary data

Supplementary material related to this article can be found, in the online version, at doi:https://doi.org/10.1016/j.jphotochem.2019.02.007.

References

[1] M. Ye, X. Gao, X. Hong, Q. Liu, C. He, X. Liu, C. Lin, Sustain. Energy Fuels 1 (2017) 1217–1231.
[2] R.J. Byers, E.R. Hitchman, Cytochem 45 (2011) 201–237.
[3] P. Alivisatos, Nat. Biotech. 22 (2004) 47–52.
[4] Y. Li, Y. Zhao, H. Cheng, Y. Hu, G. Shi, L. Dai, L. Qu, J. Am. Chem. Soc. 134 (2011) 156–166.
[5] M.S. Salman, A. Riaz, A. Iqbal, S. Zulfiqar, M.I. Sarwar, S. Shabbir, Mater. Des. 131 (2017) 156–166.
[6] A. Imamog, D.D. Awschalom, G. Burkard, D.P. DiVincenzo, D. Loss, M. Sherwin, A. Small, Phys. Rev. Lett. 83 (1999) 4204–4207.
[7] W. Yan, Q. Liu, C. Wang, X. Yang, T. Yao, J. He, Z. Sun, Z. Pan, F. Hu, Z. Wu, J. Am. Chem. Soc. 136 (2014) 1150–1155.
[8] X. Zhang, Y. Zhang, Y. Wang, S. Kalytchuk, S.V. Kershaw, Y. Wang, P. Wang, T. Zhang, Y. Zhao, H. Zhang, ACS. Nano 7 (2013) 11234–11241.
[9] K. Gugula, A. Szydlo, L. Stegemann, C. Strassert, M. Bredol, J. Mater. Chem. C 4 (2016) 5263–5269.
[10] S. Rühle, M. Shalom, A. Zaban, ChemPhysChem 11 (2010) 2290–2304.
[11] M. Ji, S. Park, S.T. Connor, T. Mokari, Y. Cui, K.J. Gaffney, Nano. Lett. 9 (2009) 1217–1222.
[12] G. Fonthal, L. Tirado-Mejıa, J. Marın-Hurtado, H. Ariza-Calderon, J. Mendoza-Alvarez, J. Phys. Chem. Solids 61 (2000) 579–583.
[13] H. Wang, L. Sun, Y. Li, X. Fei, M. Sun, C. Zhang, Y. Li, Q. Yang, Langmuir 27 (2011) 11609–11615.
[14] J. Jie, W. Zhang, I. Bello, C.-S. Lee, S.-T. Lee, Nano. Today 5 (2010) 313–336.
[15] K. Han, M. Wang, S. Zhang, S. Wu, Y. Yang, L. Sun, Chem. Commun. 51 (2015) 7008–7011.
[16] L. Tong, F. Qiu, T. Zeng, J. Long, J. Yang, R. Wang, J. Zhang, C. Wang, T. Sun, Y. Yang, RSC Adv. 7 (2017) 47999–48018.
[17] Z. Tang, N.A. Kotov, M. Giersig, Science 297 (2002) 237–240.
[18] A.F. Morais, I.G. Silva, S.P. Sree, F.M. de Melo, G. Brabants, H.F. Brito, J.A. Martens, H.E. Toma, C.E. Kirschhock, E. Breynaert, Chem. Commun. 53 (2017) 7341–7344.
[19] I. Yildiz, E. Deniz, F.M. Raymo, Chem. Soc. Rev. 38 (2009) 1859–1867.
[20] U. Kusebauch, S.A. Cadamuro, H.J. Musiol, M.O. Lenz, J. Wachtveitl, L. Moroder, C. Renner, Angew. Chem. Int. Ed. 45 (2006) 7015–7018.
[21] M. Yamada, M. Kondo, J.i. Mamiya, Y. Yu, M. Kinoshita, C.J. Barrett, T. Ikeda, Angew. Chem. Int. Ed. 47 (2008) 4986–4988.
[22] M.M. Russew, S. Hecht, Adv. Mater. 22 (2010) 3348–3360.
[23] R. Siewertsen, H. Neumann, B. Buchheim-Stehn, R. Herges, C. Näther, F. Renth, F. Temps, J. Am. Chem. Soc. 131 (2009) 15594–15595.
[24] A.A. Beharry, G.A. Woolley, Chem. Soc. Rev. 40 (2011) 4422–4437.
[25] T. Fukaminato, T. Sasaki, T. Kawai, N. Tamai, M. Irie, J. Am. Chem. Soc. 126 (2004) 14843–14849.
[26] K. Matsuda, M. Irie, J. Photochem. Photobiol. C: Photochem. Rev. 5 (2004) 169–182.
[27] H. Javed, K. Fatima, Z. Akhter, M.A. Nadeem, M. Siddiq, A. Iqbal, Proc. R. Soc. A 472 (2016) 20150692/1-12.
[28] S. Saeed, P.A. Channar, F.A. Larik, A. Saeed, M.A. Nadeem, A. Iqbal, J. Photochem. Photobiol. A: Chem. 371 (2019) 44–49.
[29] T. Hansen, K. Žídek, K. Zheng, M. Abdellah, P. Chábera, P. Persson, T. Pullerits, J. Phys. Chem. Lett. 5 (2014) 1157–1162.
[30] J.S. Mak, A.A. Farah, F. Chen, A.S. Helmy, ACS Nano 5 (2011) 3823–3830.
[31] G. Shabir, A. Saeed, P.A. Channar, F.A. Larik, T.A. Fatah, J. Fluoresc. 27 (2017) 2213–2221.
[32] M. Shen, W. Jia, Y. You, Y. Hu, F. Li, S. Tian, J. Li, Y. Jin, D. Han, Nanoscale Res. Lett. 8 (2013) 253/1-6.
[33] W.W. Yu, L. Qu, W. Guo, X. Peng, Chem. Mater. 15 (2003) 2854–2860.
[34] M. Iqbal, M.A.Z.G. Sial, S. Shabbir, M. Siddiq, A. Iqbal, J. Photochem. Photobiol. A: Chem. 335 (2017) 112–118.
[35] A.A. Beharry, O. Sadovski, G.A. Woolley, J. Am. Chem. Soc. 133 (2011) 19684–19687.
[36] P.A. Gale, C. Caltagirone, Coord. Chem. Rev. 354 (2018) 2–27.
[37] I. Yildiz, M. Tomasulo, F.M. Raymo, J. Mater. Chem. 18 (2008) 5577–5584.
[38] P. Moroz, Z. Jin, Y. Sugiyama, D.A. Lara, N. Razgoniaeva, M. Yang, N. Kholmicheva, D. Khon, H. Mattoussi, M. Zamkov, ACS. Nano 12 (2018) 5657–5665.
[39] A. Iagatti, L. Tarpani, E. Fiacchi, L. Bussotti, A. Marcelli, P. Foggi, L. Latterini, Photochem. Photobiol. Sci. 14 (2015) 397–406.
[40] S. Bhattacharyya, B. Paramanik, S. Kundu, A. Patra, ChemPhysChem 13 (2012) 4155–4162.
[41] V. Muhr, C. Würth, M. Kraft, M. Buchner, A.J. Baeumner, U. Resch-Genger, T. Hirsch, Anal. Chem. 89 (2017) 4868–4874.
[42] K. Zheng, K. Zidek, M. Abdellah, N. Zhu, P. Chábera, N. Lenngren, Q. Chi, Tn. Pullerits, J. Am. Chem. Soc. 136 (2014) 6259–6268.